Enhancing Hydrogenotrophic Methanation in a Bentonite-Amended Bubble Reactor Under Mesophilic Conditions

Apostolos Spyridonidis and Katerina Stamatelatou *

Posted Date: 24 February 2026

doi: 10.20944/preprints202602.1438.v1

Keywords: biogas upgrade; biomethane; hydrogenotrophic methanogenesis; bubble reactor; bentonite

 doi:10.20944/preprints202602.1438.v1

Article

Enhancing Hydrogenotrophic Methanation in a Bentonite-Amended Bubble Reactor Under Mesophilic Conditions

Apostolos Spyridonidis and Katerina Stamatelatou *

Department of Environmental Engineering, Democritus University of Thrace, Vas. Sophias 12, GR-67132 Xanthi, Greece

* Correspondence: astamat@env.duth.gr; Tel.: +30-2541079315

Abstract

This study explores the use of bentonite to enhance biological biogas upgrading in a bubble reactor (BR) operated under mesophilic conditions (39 ± 1 °C). The experimental setup consisted of a 2 L vertically oriented BR (height to diameter ratio 16:1) fed with a synthetic gas mixture (60% H_2, 15% CO_2, 25% CH_4, v/v) at a gas recirculation rate of 4 L L_R^{-1} h^{-1}. The aim was to overcome hydrogen's low gas-liquid mass transfer rate while avoiding the operational challenges typically associated with trickle-bed reactors (TBRs). Bentonite increases the density and hydrostatic pressure of the liquid medium, and likely alters its rheology, thereby extending the gas-liquid contact time without requiring elevated pressures or intensive gas recirculation. Additionally, bentonite is expected to provide microstructural support that promotes the formation of biofilm-like communities, creating favorable microenvironments for hydrogenotrophic methanogens. As a clay-based additive, bentonite may also contribute to improved process stability through adsorption of inhibitory compounds, enhanced biomass retention, and pH buffering. Under mesophilic conditions, the bentonite-modified BR achieved a methane production rate of 2.17 ± 0.06 L $_{CH4}$ L_R^{-1} d^{-1} at a gas retention time of 1.49 h, with methane purity reaching 96.25%. In comparison, a previously reported mesophilic BR operated under identical reactor configuration and operating conditions but without bentonite exhibited substantially lower methane production rates, supporting the beneficial role of bentonite in biological methanation. The findings highlight bentonite's potential dual role -physical and biological- in improving process efficiency and stability in biological methanation.

Keywords: biogas upgrade; biomethane; hydrogenotrophic methanogenesis; bubble reactor; bentonite

1. Introduction

Biomethane is a renewable gas similar in composition to natural gas but derived from biomass, such as animal waste, food waste, agro-industrial residues, and urban sludge [1]. Unlike natural gas, a non-renewable fossil fuel, biomethane is produced by upgrading biogas from anaerobic digestion, a standard method for treating organic waste [2]. Biogas typically consists of 50-70% methane (CH_4) and 30-50% carbon dioxide (CO_2) [3]. The methane content depends on the carbon oxidation state of the feedstock and the reactor's mixed-liquid alkalinity.

Biomethane production through the biological route, classified explicitly as second-generation upgrading, involves a biochemical process in which CO_2 in biogas is combined with hydrogen (H_2) by hydrogenotrophic methanogens, generating CH_4 [4,5]. H_2 is produced by water electrolysis, a method that harnesses surplus electricity generated during off-peak periods by renewable energy sources, such as solar and wind farms. In this way, surplus renewable energy can be effectively converted into a storable fuel [3,6]. One of the standout advantages of biomethane is its compatibility with the existing natural gas infrastructure. This characteristic enables efficient storage and transport

 doi:10.20944/preprints202602.1438.v1

of biomethane from rural production sites, where organic waste is typically converted into biogas, to urban centers with significantly higher energy demand [7,8]. Furthermore, the potential of biomethane as a viable substitute for conventional natural gas offers compelling benefits. These include a reduction in dependence on traditional natural gas suppliers, making energy more affordable due to the generally lower production costs of biomethane, the substantial reduction in greenhouse gas (GHG) emissions associated with fossil fuel use, and an enhancement of waste management practices by transforming organic waste into a valuable resource for energy production [9,10].

Biological upgrading of biogas can be implemented in two configurations: within the same bioreactor as part of anaerobic digestion or in a separate reactor. The former approach, known as the "in-situ process", involves injecting H_2 directly into the anaerobic digestion reactor. This injection promotes CO_2 consumption, thereby increasing the calorific value of biogas through enhanced CH_4 production [11]. This method is potentially cost-effective, as it eliminates the need for an additional reactor dedicated to biomethane production. However, this process requires careful and continuous monitoring of various operational parameters to maintain efficiency and prevent disruptions [12,13]. One significant challenge of the in-situ process is that CO_2 consumption can raise the reactor pH above 8.5. Such an increase in pH may adversely affect the overall anaerobic digestion process [14]. Moreover, under high H_2 partial pressure, the degradation of volatile fatty acids (VFAs) through acetogenesis isn't favored thermodynamically. VFAs accumulation may impair the acetoclastic methanogenesis pathway and lead to process inhibition [12]. Alternatively, in the ex-situ method, H_2 and CO_2 are introduced into a reactor inoculated with hydrogenotrophic archaea. Separating the two processes appears to enhance both their operational stability and overall efficiency [15]. Such optimized conditions enable the ex-situ method to achieve significantly higher methane productivity, often exceeding 95% methane content in the biogas, compared with the in-situ approach [1,16].

For the biological upgrading process to evolve effectively, H_2 must transition from the gas phase into the liquid phase, where hydrogenotrophic methanogenesis occurs. One of the major obstacles hindering this process is the extremely low gas-liquid mass transfer rate of H_2, a challenge mainly due to its poor solubility in water [13,17]. To overcome this constraint, researchers have explored various bioreactor types and strategies to enhance H_2 transfer. For example, vigorous mixing techniques have been employed in Continuous Stirred Tank Reactors (CSTRs) [18], intensive recirculation rates have been studied in Bubble Reactors (BRs) [19], specialized diffusers with fine pore sizes have been used [20], elevated pressure to increase solubility has been applied [21], and packing materials have been incorporated to increase the interface area of biofilm and gaseous phase in upflow reactors [22]. All these efforts led to substantial improvements in the performance of biological biogas upgrading. The use of packing material is essential in an innovative reactor design, the Trickle Bed Reactor (TBR). A TBR features a tall cylindrical column filled with packing material that fosters biofilm formation, enriched primarily by hydrogenotrophic methanogens [9,23]. This reactor design concept significantly increases the interface between gaseous substrates and methanogens [15]. As a result of these advantages, TBRs have consistently demonstrated markedly higher biomethanation rates in ex-situ biogas upgrading processes than homogeneous configurations, such as CSTRs or BRs [24,25].

While TBRs are recognized for their high efficiency in gas-liquid mass-transfer processes, several operational and economic challenges may hinder their practical implementation for biological biogas upgrading. Although clogging from excessive biofilm growth is considered a drawback of packed-bed systems, this issue appears less critical in TBRs operated under autotrophic methanogenic conditions, due to the relatively low growth rates of hydrogenotrophic methanogens. Indeed, studies by Burkhard et al.[26] and Karyofyllidou et al [27], conducted under mesophilic conditions, did not observe operational problems due to clogging. Instead, the performance of TBRs is strongly influenced by the hydrodynamic behavior of both the trickling liquid stream and the gases rising, as well as by parameters such as liquid hold-up, bed void fraction, and the degree of biofilm wetting [28,29]. Inadequate wetting or non-uniform flow distribution can substantially reduce biological activity and effective mass transfer. Furthermore, the performance of TBRs is linked to the specific surface area and the physicochemical characteristics of the packing material, which influence the

 doi:10.20944/preprints202602.1438.v1

microbial attachment and the essential gas-liquid interactions that drive the conversion process [15]. Much of the existing research has relied on commercially manufactured materials, which may entail higher costs, thereby limiting the economic feasibility of scaling these processes.

The primary objective of this study is to address the very low gas-liquid mass transfer rate of H_2 and to optimize BR performance, thereby avoiding the technical issues associated with TBRs. The exceptionally low gas-liquid mass transfer rates for hydrogen significantly hamper the performance of BRs, despite their simple design. In these reactors, gaseous substrates are introduced at the bottom through a diffuser, creating discrete bubbles that ascend through the liquid medium. This rapid upward movement of bubbles results in a relatively short residence time for the gases in the reactor, typically a few minutes. Such limited contact time between microorganisms and gaseous substrates limits the overall conversion efficiency of the process, as highlighted by [30]. Previous strategies to enhance this contact time have primarily focused on increasing gas recirculation rates. While this approach improves mass transfer efficiency, as described by Kougias et al. [19], it comes at the cost of significant energy consumption, which can undermine the process's economic feasibility. In the current study, a novel approach was employed by incorporating bentonite clay into the reactor to increase the liquid phase density. Bentonite was added to increase the viscosity of the liquid phase and to increase hydrostatic pressure in the column. This modification effectively prolonged the bubble ascent time in the reactor, thereby extending the contact time between the gaseous substrates and the microorganisms. Prior investigations have shown that elevated pressures in TBRs can significantly enhance biomethanation performance, as demonstrated by Ullrich et al. [26,31]. However, these studies have typically explored pressure levels ranging from 2 bar to 9 bar—conditions that may not justify the substantial capital investments required, as the authors state. In contrast, a simple approach is employed herein by integrating bentonite into the process to achieve modest pressure increases.

The inclusion of inert or packing materials in homogeneous bioreactors introduces controlled micro-scale heterogeneity, which paradoxically enhances the overall homogeneity of function. The attached microorganisms self-organize into biofilm communities that establish localized microenvironments with gradients in substrate concentration and redox potential. These gradients foster ecological niches that support syntrophic interactions and metabolic complementarity among species, thereby improving substrate conversion efficiency and system robustness [32]. Moreover, bentonite isn't completely inert in a physical sense, as it exhibits physicochemical activity that can influence microbial performance and reactor chemistry in subtle yet meaningful ways. Previous studies have shown that bentonite, as well as other clay-based additives, can absorb inhibitory compounds such as ammonium, promote biomass retention, and buffer pH, thereby improving process stability [33,34]. Finally, this study explicitly examines the mesophilic temperature range, which typically exhibits slower microbial kinetics than the more favorable thermophilic conditions associated with higher biogas production rates [18,35], while aiming to improve the process performance.

Therefore, the addition of bentonite in the BR is proposed to enhance bubble-liquid interactions and, consequently, gas-liquid mass transfer, contributing to the high methane production rates observed under mesophilic conditions. Previous anaerobic digestion studies have demonstrated that bentonite can improve methane yield and process stability through buffering and adsorption effects [34,36,37]. Together with the present results, these findings suggest that bentonite-enriched BRs may represent a viable and operationally simple alternative for efficient biological biogas upgrading under mesophilic conditions. For comparison, the performance of the bentonite-enriched BR is evaluated against a previously reported mesophilic BR operated under the same reactor configuration and conditions [25].

2. Materials and Methods

2.1. Inoculum and Nutrient Media

The digestate used in this study was sourced from a full-scale biogas reactor predominantly fed with cow manure and corn silage, operating at 40 °C under mesophilic conditions. The full-scale anaerobic digester operated with a hydraulic retention time of 27 d and an organic loading rate of

 doi:10.20944/preprints202602.1438.v1

3.15 gVS/L_R^{-1} d^{-1}. The digester was producing approximately 1.35 L_{CH4} L_R^{-1} d^{-1}, without any sign of inhibition, which is confirmed by the absence of VFAs. To prepare the inoculum, the raw digestate was sieved through a 2mm mesh screen. This step was crucial for eliminating coarse particulate matter, ensuring a consistent, homogeneous sample. Following sieving, the filtered digestate was combined with bentonite clay to increase solid concentration. The mixing process continued until a uniform semi-solid mixture was achieved, essential for maintaining stable conditions during the experiments. The ratio of bentonite to digestate was carefully calibrated to reach an initial total solids (TS) concentration of approximately 220 g L_R^{-1}.

The bentonite used in this study was montmorillonite-rich, commercially available from Italy, and was supplied by Syndesmos, Greece. The material consisted mainly of montmorillonite (≥80% w/w, dry basis), with a specific surface adsorption capacity ≥300 mg 100 g^{-1} (Table A1). The pH of a 5% aqueous dispersion was measured at 9.23, indicating a mild alkaline buffering capacity. The loss on drying was approximately 11%. Particle size distribution data indicated that ≤10% of particles were below 10 μm, while the crystalline silica content was ≤3%. These properties align with those of a swelling, high-surface-area smectite clay, typically used for adsorption, buffering, and rheological modification in aqueous systems [38–41].

The compositional characteristics of the inoculum before and after the incorporation of bentonite are detailed in Table 1. A detailed characterization of the inoculum is given in Table A2. Since all required macro- and micronutrients were provided through the digestate, no additional synthetic nutrient medium was supplied, consistent with other studies that used digestate as inoculum [12,42].

Table 1. Characteristics of digestate before and after bentonite addition.

Parameters	Before bentonite addition	After bentonite addition
pH	7.78	7.94
Cond (mS cm^{-1} @25°C)	17.98	16.74
TS (%)	3.29	21.93
VS (%)	2.61	2.30

2.2. Experimental Setup and Operation

The BR setup consisted of a single, vertically oriented borosilicate glass column with a working volume of 2 L and a gas-phase capacity of 0.9 L. The column's internal diameter was 5.5 cm, and its height was 105 cm, resulting in a height-to-diameter ratio of approximately 16:1, comparable to or higher than most values reported in the literature [30,43,44] (Figure 1).

To initiate the process, the BR was inoculated with 2 L of a mixed digestate that incorporated bentonite. The feeding gas mixture was composed of H_2 at 60% v/v, CO_2 at 15% v/v, and CH_4 at 25% v/v. This H_2:CO_2 ratio of 4:1 is stoichiometric for the complete conversion of gaseous substrates to methane. Moreover, the 60:40 CH_4:CO_2 ratio simulates the typical composition of raw biogas.

The gas-feeding mixture was contained within gas-tight aluminum bags to prevent leakage. It was continuously introduced into the BR via a commercially available gas diffuser and a precise peristaltic pump (as illustrated in Figure 1). To maximize gas-liquid contact and optimize mass transfer efficiency, continuous gas recirculation was employed at a flow rate of 4 L L_R^{-1} h^{-1}. The produced biomethane was also collected and stored in gas-tight aluminum bags for subsequent analysis.

To ensure anaerobic conditions were established in the reactor, a nitrogen (N_2) purge was conducted at the beginning of the operation. Maintaining a stable temperature was critical, as even slight decreases below the set operating value can slow microbial kinetics. For this reason, the reactor environment was maintained at 39 ± 1 °C using a flexible heating tape controlled by a temperature controller. This temperature corresponds to typical mesophilic anaerobic digestion conditions.

To foster microbial activity, 50 mL of the bentonite-enriched digestate was added bi-weekly to the BR to ensure the availability of essential nutrients in the digestate. Importantly, before adding the bentonite, the digestate was degassed to remove residual biogas, thereby avoiding any influence on the biomethane composition. The bentonite-enriched digestate used as the nutrient medium was prepared following the same procedure applied for inoculum preparation.

 doi:10.20944/preprints202602.1438.v1

A second BR, whose performance had previously been reported by the same authors [25], was used as a reference in the present study. This reactor consisted of a borosilicate glass column identical in height, internal diameter, and working volume to the bentonite-enriched BR. The reactor was continuously supplied with the same synthetic gas mixture (CH_4 60% v/v, CO_2 15% v/v, and CH_4 25% v/v) through an identical diffuser and operated at the same gas recirculation rate of 4 L L_R^{-1} h^{-1}. Both reactors were inoculated with digestate from the same biogas plant, while the reference BR had previously been operated under hydrogenotrophic conditions, resulting in a microbial community with higher initial methanogenic activity.

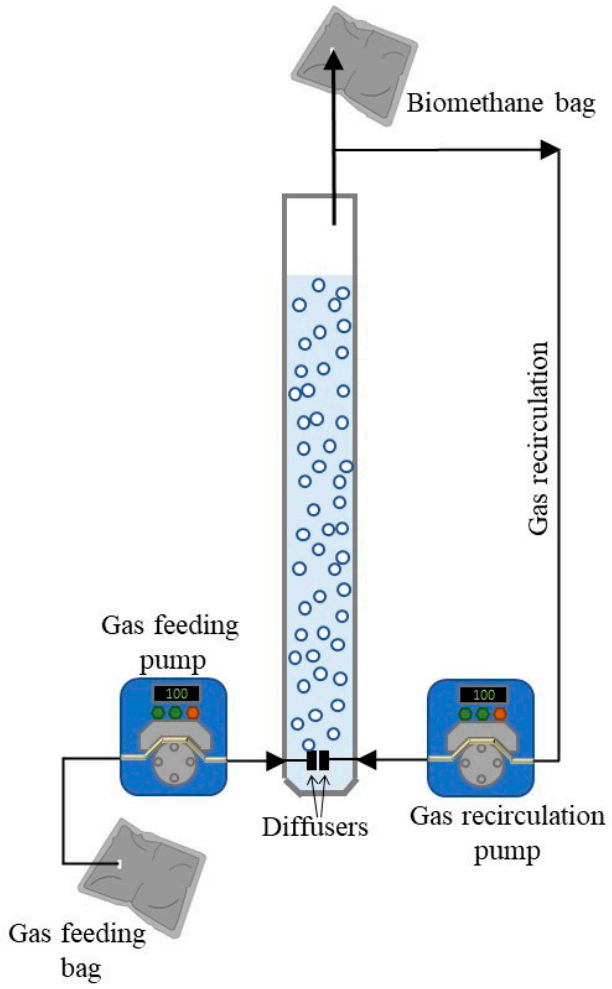

Figure 1. Schematic depiction of bubble reactor setup.

Analytical methods and calculations

Total solids (TS), volatile solids (VS), pH, and electrical conductivity were determined according to Standard Methods for the Examination of Water and Wastewater (APHA 2023) [34]. Specifically, pH and electrical conductivity (EC) were measured using a digital pH and electrical conductivity (EC) meter from HANNA Instruments (HI 83141). Liquid samples were collected from the BR weekly. The concentrations of volatile fatty acids (VFAs) and the gas composition were determined by gas chromatography. A comprehensive description of the methodology is provided in Appendix B. Gas volume was calculated based on the displacement of an equivalent volume of acidified aqueous solution at 20 °C, the ambient temperature during the experiment.

The hydrogen loading rate (HLR; L L_R^{-1} d^{-1}) was calculated as the hydrogen volume introduced into the bioreactor per unit of reactor working volume per unit of time. It was determined based on the total gas loading rate (GLR) and the volumetric fraction of H_2 (%) in the feed gas mixture (H_{2in}), as described by Equation 1.

 doi:10.20944/preprints202602.1438.v1

$$\mathrm{HLR} = \mathrm{H_{2_{in}}} \cdot \mathrm{GLR} \quad (1)$$

The net Methane Production Rate (Net MPR; L L_R^{-1} d^{-1}) was defined according to equation 2, where MPR (L L_R^{-1} d^{-1}) and MLR (L L_R^{-1} d^{-1}) are the Methane Production and Loading Rates, respectively.

$$\mathrm{Net\ MPR} = \mathrm{MPR} - \mathrm{MLR} \quad (2)$$

The H_2 utilization efficiency (%) was estimated based on equation 3, where HLR (L L_R^{-1} d^{-1}) and HOR (L L_R^{-1} d^{-1}) are the H_2 Loading and Outlet Rates, respectively.

$$\eta_{H_2} = \frac{\mathrm{HLR} - \mathrm{HOR}}{\mathrm{HOR}} \cdot 100 \quad (3)$$

The utilization efficiency of CO_2 (%) was determined similarly according to equation 5.4, where CLR (L L_R^{-1} d^{-1}) and COR (L L_R^{-1} d^{-1}) are the CO_2 Loading and Outlet Rates, respectively.

$$\eta_{CO_2} = \frac{\mathrm{CLR} - \mathrm{COR}}{\mathrm{CLR}} \cdot 100 \quad (4)$$

The pressure at the bottom of the BR was estimated based on the determined slurry density using a simple hydrostatic model (Eq. 5). This expression is derived from the general axial pressure balance in a gas-liquid-solid column by assuming steady-state conditions, negligible acceleration, and homogeneous liquid-solid mixture along the column. Since the variations in the solids' concentration could not be captured, the final calculated value (1.13 bar at the bottom) should be considered an approximate indication of the order of magnitude of the pressure developed at the bottom of BR. The analytical calculations are presented in Appendix B.

$$P = P_{atm} + \rho_{sl} \cdot g \cdot h \quad (5)$$

3. Results

The experimental period spanned 165 days and was divided into 13 distinct phases, each defined by the specific gas retention time (GRT) implemented. Initially, the GRT was 23 h; this duration was progressively reduced by increasing the feeding gas loading rate until a notable decline in biogas reactor (BR) performance was observed. During the initial stages of operation, particularly during the first four days, a pronounced lag phase was observed in the biogas reactor's performance. On day 4, the content of CH_4 in the gas effluent was recorded at a mere 62% (as illustrated in Figure 2). This initial low methane concentration can be attributed to the biomass inoculum, sourced from a biogas production facility that lacked enrichment for hydrogenotrophic methanogens. Furthermore, the pre-treatment step of allowing the biomass to degas was likely a contributing factor to the initial lag. This process was designed to remove residual biogas that could interfere with the reactor's microbial dynamics. However, by day 6, a significant turnaround occurred, with methane content rising above 95%. This rapid increase indicated the rapid adaptation of the biomass to the modified operational conditions, highlighting the potential for improved biogas production.

 doi:10.20944/preprints202602.1438.v1

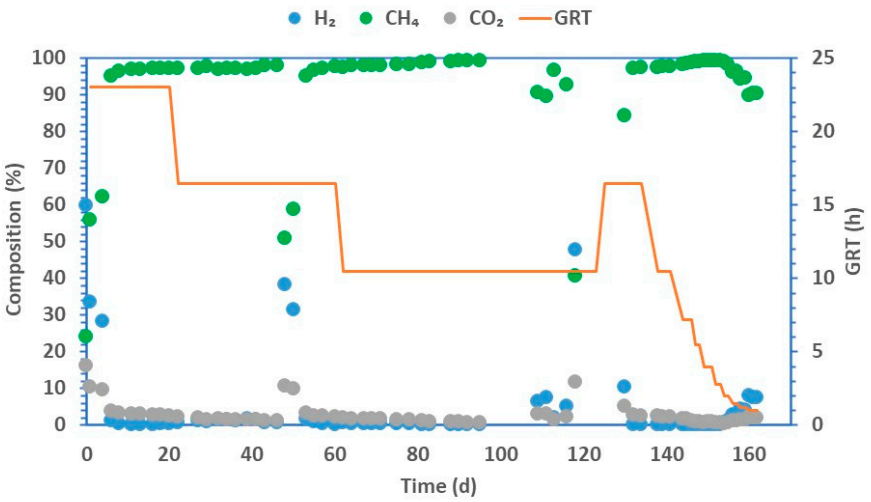

Figure 2. Biomethane gas composition.

Once a stable operational state was established, the GRT in the bioreactor was gradually reduced from 16 to 10.5 h. With this adjustment, the BR performed well, with CH_4 concentrations in the biogas exceeding 95%. However, on day 48, an unexpected failure of the feeding pump caused a complete shutdown for an entire day, resulting in a noticeable decline in reactor performance upon resumption of operation. Despite this setback, the biomethanation process recovered quickly, and within three days the methane content of the produced biomethane rebounded to 95%. A similar event occurred on day 99 when another malfunction in the pump's functionality was recorded. The repair process proved ineffective, prompting the decision to replace the pump entirely on day 125. The GRT was deliberately increased to 16 h to mitigate potential shock to the microbial community and to avert the risk of acetic acid accumulation via the acetogenic pathway, as suggested by Agneessens et al. [7].

By day 132, biomethanation performance had fully recovered, with methane concentrations reaching 97.10%. This successful recovery underscored the resilience of the microbial ecosystem within the bioreactor, despite operational challenges. Following the initial phase of the experiment, the GRT was systematically reduced until it reached a minimum threshold of 0.99 h. Across the GRT conditions tested, at 7.19, 5.48, 3.97, 2.81, and 1.98 h, the efficiency of biomethanation remained high, with CH_4 concentration consistently exceeding 98.50%. This sustained performance indicates a stable and effective anaerobic digestion process under these conditions.

The net MPR experienced a significant increase, rising from an average of 0.26 ± 0.03 to 1.81 ± 0.16 L_{CH4} L_R^{-1} d^{-1}. Additionally, the H_2 conversion rate remained remarkably high, above 99%, as illustrated in Figure 3. However, when the GRT was further reduced from 1.98 to 1.49 h, a slight decrease in methane concentration was detected, averaging at 96.25 ± 0.05%. Despite this decline in purity, the net MPR continued to increase, reaching 2.17 ± 0.06 L_{CH4} L_R^{-1} d^{-1}. As the GRT was pushed to even lower values - specifically 1.19 and 0.99 h - there was a marked deterioration in the quality of the produced biomethane. The CH_4 content dropped significantly to 90.24 ± 0.33%. This reduction correlated with a decrease in the net MPR, which fell to 1.91 ± 0.08 L_{CH4} L_R^{-1} d^{-1} (Table 2).

 doi:10.20944/preprints202602.1438.v1

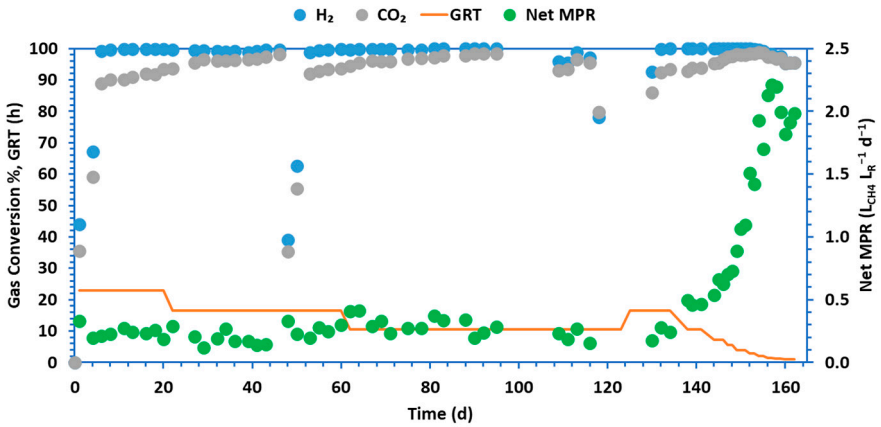

Figure 3. Utilization efficiencies of gaseous substrates and net MPR.

Comparing the BR studied herein with the reference BR [25] shows that even at the higher GRT (23 h), the bentonite-enriched reactor achieved a net MPR of 0.23 ± 0.04 L CH_4 L_R^{-1} d^{-1}, significantly higher than the 0.08 ± 0.04 CH_4 L_R^{-1} d^{-1} recorded for the reference BR (Table 2). When the GRT was reduced to 16.4h, the performance of both BRs was approximately the same, although the bentonite-enriched BR continued to exhibit a slightly higher net MPR. A further reduction in GRT to 10.5h led to a substantial performance divergence. The bentonite-enriched BR reached a net MPR of 0.47 ± 0.06 L CH_4 L_R^{-1} d^{-1}, while the reference BR net MPR was increased only slightly, from 0.21 ± 0.03 to 0.27 ± 0.02 L CH_4 L_R^{-1} d^{-1}. At this operating GRT, a significant difference in CH_4 content between the two systems was observed, with the bentonite-amended BR achieving 97.71 ± 0.15 % CH_4 compared to 91.15 ± 1.01 % in the reference reactor. Finally, by increasing the Hydrogen Loading Rate (HLR) to approximately 2 L H_2 L_R^{-1} d^{-1}, corresponding to a GRT of 7.2 h, the bentonite-enriched BR demonstrated a net MPR almost twice that of the reference (Table 2). Notably, despite the increased HLR, the net MPR of reference BR remained the same at 0.27±0.06 L CH_4 L_R^{-1} d^{-1}. This increase in HLR was accompanied by a substantial decline in CH_4 content in the reference reactor from 91.15 ± 1.01 % to 65.01 ± 7.05 %, indicating process instability. In contrast, the CH_4 content in bentonite-amended BR increased slightly, from 97.71 ± 0.15 % to 98.43 ± 0.31%, demonstrating the system's robustness.

The incorporation of bentonite increased the density and apparent viscosity of the mixed liquor, thereby modifying the hydrodynamic behavior of the reactor. Reduced bubble rise velocity and increased gas holdup were visually observed relative to the reference bubble reactor operated under identical conditions [25]. While bubble size or volumetric mass transfer coefficient (k_La) were not directly quantified, the higher methane production rates and improved H_2 and CO_2 utilization efficiencies at the same gas retention time strongly suggest enhanced gas–liquid mass transfer in the bentonite-enriched system.

Table 2. Bubble reactor efficiency for each studied GRT (values in parentheses denote the standard deviation).

Phase	I	II	III	IV	V	VI	VII	VIII	IX	X	XI	XII	XIII
GRT (h)	23.02	16.44	10.46	16.44	10.46	7.19	5.48	3.97	2.81	1.98	1.49	1.19	0.99
HLR (L_{H2} $L_R^{-1}d^{-1}$)	0.62	0.86	1.36	0.86	1.36	1.97	2.59	3.58	5.06	7.16	9.50	11.97	14.32
CH_4 (%)	97.14 (0.06)	97.14 (0.53)	92.95 (3.48)	97.31 (0.29)	97.71 (0.15)	98.43 (0.31)	99.03 (0.07)	99.22 (0.03)	99.33 (0.11)	98.58 (0.59)	96.25 (0.05)	94.50 (0.13)	90.24 (0.33)
CH_4^R (%)	92.24 (0.36)	94.63 (0.15)			91.15 (1.01)	65.01 (7.05)							

 doi:10.20944/preprints202602.1438.v1

H_2 (%)	0.25 (0.11)	0.47 (0.36)	4.85 (2.81)	0.07 (0.10)	0.02 (0.00)	0.03 (0.05)	0.00 (0.00)	0.01 (0.01)	0.06 (0.08)	0.88 (0.51)	2.67 (0.04)	4.14 (0.11)	7.67 (0.27)
H_2^R (%)	4.92 (0.34)	2.38 (0.16)			4.93 (1.08)	27.1 (5.61)							
CO_2 (%)	2.61 (0.13)	2.39 (0.18)	2.20 (0.68)	2.62 (0.18)	2.28 (0.15)	1.54 (0.27)	0.97 (0.07)	0.77 (0.03)	0.62 (0.03)	0.54 (0.08)	1.08 (0.01)	1.36 (0.02)	2.09 (0.06)
CO_2^R (%)	2.84 (0.08)	2.99 (0.06)			3.92 (0.31)	7.88 (1.46)							
ηH_2 (%)	99.81 (0.08)	99.65 (0.27)	97.17 (1.65)	99.95 (0.08)	99.99 (0.00)	99.98 (0.03)	100.0 (0.00)	100.0 (0.00)	99.96 (0.06)	99.43 (0.32)	98.26 (0.01)	97.49 (0.12)	95.49 (0.13)
ηH_2^R (%)	94.81 (1.90)	98.53 (0.2)			96.53 (0.88)	77.57 (5.96)							
ηCO_2 (%)	92.34 (0.92)	93.33 (0.38)	95.12 (1.50)	92.89 (0.82)	93.44 (0.58)	95.85 (0.65)	97.52 (0.17)	97.99 (0.16)	98.39 (0.06)	98.65 (0.16)	97.34 (0.01)	96.88 (0.12)	95.37 (0.11)
ηCO_2^R (%)	92.49 (1.04)	93.11 (1.37)			89.83 (0.7)	75.88 (5.9)							
MPR (L_{CH_4} $L_R^{-1}d^{-1}$)	0.48 (0.04)	0.62 (0.03)	0.74 (0.06)	0.60 (0.03)	1.01 (0.02)	1.39 (0.06)	1.75 (0.02)	2.44 (0.11)	3.48 (0.06)	4.66 (0.16)	5.95 (0.06)	6.86 (0.14)	7.60 (0.08)
MPR^R	0.37 (0)	0.57 (0.03)			0.73 (0.02)	1.07 (0.06)							
Net MPR (L_{CH_4} $L_R^{-1}d^{-1}$)	0.23 (0.04)	0.28 (0.03)	0.20 (0.06)	0.26 (0.03)	0.47 (0.02)	0.61 (0.06)	0.71 (0.02)	1.02 (0.11)	1.46 (0.06)	1.81 (0.16)	2.17 (0.06)	2.10 (0.14)	1.91 (0.08)
Net MPR^R (L_{CH_4} $L_R^{-1}d^{-1}$)	0.08 (0.04)	0.21 (0.03)			0.27 (0.02)	0.27 (0.06)							

Superscript R denotes the results of the reference reactor [25].

Based on these observations, the optimal HLR for the bentonite-enriched bioreactor was identified as 9.50 L_{H_2} L_R^{-1} d^{-1}, whereas the reference reactor exhibited an optimal HLR of 0.86 L_{H_2} L_R^{-1} d^{-1}. Operation beyond these optimal values led to a marked decline in reactor performance, as evidenced by reductions in both methane purity and the volumetric methane production rate. The strong dependence of net MPR on HLR is illustrated in Figure 4, which shows a clear downward trend in net MPR when the HLR exceeds 9.50 L H_2 L_R^{-1} d^{-1}.

 doi:10.20944/preprints202602.1438.v1

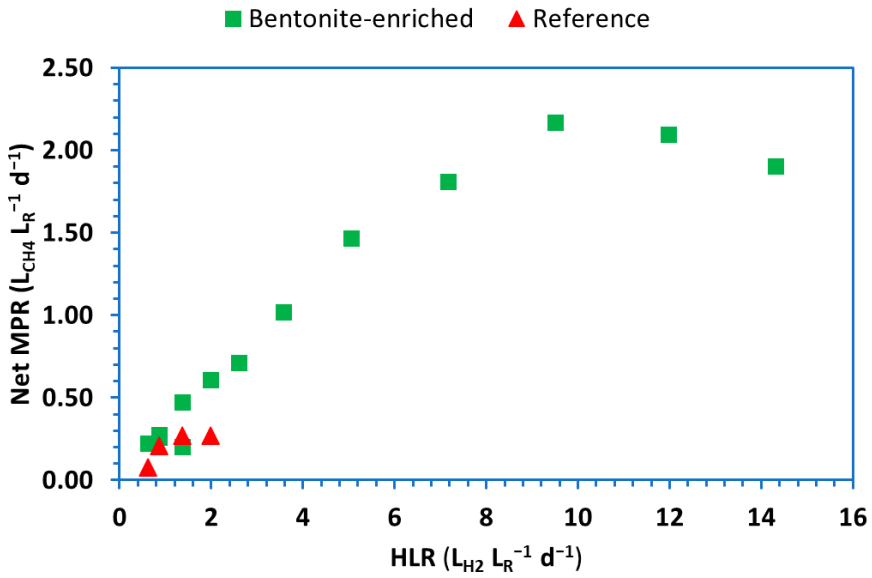

Figure 4. Net Methane Production rate vs Hydrogen Loading rate.

The pH levels within the bentonite-enriched reactor increased from 7.90 to approximately 8.30 (see Figure 5). Similarly, the pH of the reference reactor increased from 7.82 to 8.00 during the start-up [25]. This shift is primarily attributed to the reduction of bicarbonate during hydrogenotrophic methanation. Despite this upward trend, the pH remained within the optimal range of 6.5 to 8.5, which is crucial for promoting efficient hydrogenotrophic methanogenesis, as highlighted by [19]. In fact, similar observations have been reported from various ex-situ biogas upgrading systems. For instance, Kamravamanesh et al. [45] documented a pH escalation from 8.0 to 8.9 in a TBR. Yet, no adverse effects on hydrogenotrophic methanogenic performance were noted, underscoring the stability of these microbial communities. Likewise, Tsapekos et al. [46] reported pH oscillations consistently between 8.0 and 8.5, a range that did not cause any decline in biomethanation efficiency, thereby validating the robustness of these microorganisms under slightly alkaline conditions. Conversely, Thapa et al. [47] observed a marked decrease in bioreactor efficiency as pH reached 8.77. To counteract this, they introduced an acidic solution, thereby stabilizing the pH within a more favorable range of 8.15-8.28. Furthermore, Huang et al. [14] observed a significant decline in biomethanation performance in a TBR when pH levels reached 9.2. To address this issue, they adjusted the H_2/CO_2 feeding ratio, successfully restoring the pH to a more manageable 8.00, thereby enhancing bioreactor performance. This pH control aligns closely with the current study's findings, underscoring the critical importance of maintaining pH below 8.5 to sustain the efficacy of hydrogenotrophic methanogenesis.

 doi:10.20944/preprints202602.1438.v1

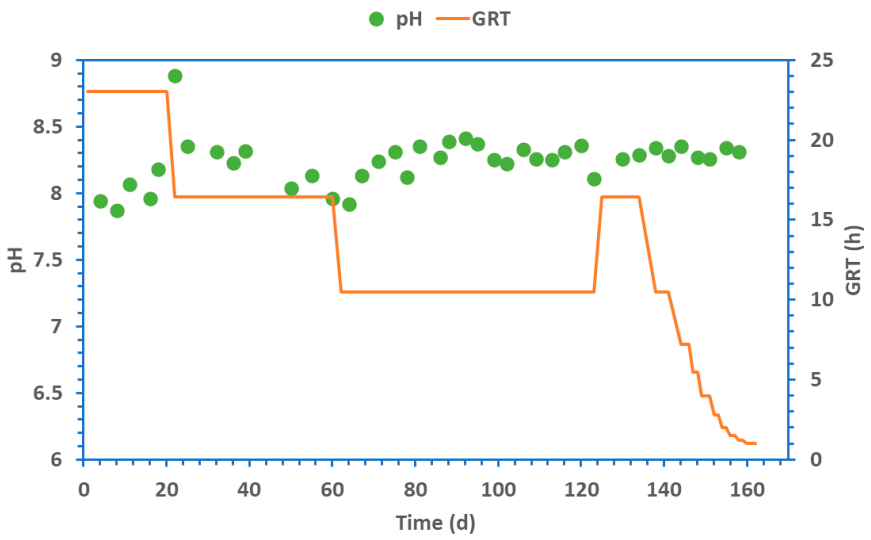

Figure 5. pH of the BRs' mixed liquor under decreasing GRTs.

Throughout the experimental period, the VFAs concentrations remained consistently below 0.01 g L_R^{-1}. Remarkably, even when the GRT was reduced to 1 h, no detectable VFA accumulation was observed in the bentonite-enriched reactor. This behavior is consistent with the stable pH values of approximately 8.3 maintained throughout the experiment. In contrast, in the reference bioreactor [25], reducing the GRT to 7.2 h resulted in rapid acetate accumulation, with concentrations reaching up to 1.5 g L_R^{-1}. This was accompanied by a pronounced decrease in pH to approximately 6.2, indicating a severe loss of process stability. The addition of Na_2CO_3 and 1 N NaOH was subsequently applied to neutralize the pH and promote microbial activity; however, the reactor did not recover, and stable biomethanation could not be re-established. Consequently, the operation of the reference reactor was terminated.

4. Discussion

The bentonite-enriched BR in this work showed enhanced biomethanation efficiency compared to the reference BR, indicating the potential of bentonite as a cost-effective additive for modifying the hydrodynamic conditions of the mixed liquor. In the reference reactor, the accumulation of VFAs - particularly acetate - was identified as the primary factor leading to performance deterioration. By contrast, the absence of VFA accumulation in the bentonite-enriched system suggests that bentonite may contribute to improved process stability and more efficient hydrogen utilization, potentially by moderating local physicochemical conditions within the reactor. The consistent outperformance of the bentonite-enriched BR across nearly all tested gas retention times indicates that the increased liquid density and associated elevation in hydrostatic pressure played a key role in enhancing methane production. Overall, these findings support the hypothesis that bentonite modifies the hydrodynamic environment of the reactor in a manner favorable for ex-situ biological biogas upgrading.

These results indicate that bentonite emerges as a promising alternative for boosting the performance of an ex-situ biogas upgrading BR. A critical challenge in these systems is enhancing hydrogen gas mass transfer into the liquid, a hurdle that previous researchers have addressed through various innovative strategies. For instance, Bassani et al. [37] meticulously examined the effectiveness of four highly efficient diffusion devices under thermophilic conditions in bioreactors. Their findings revealed a remarkable net MPR of 0.82±0.15 L_{CH4} L_R^{-1} d^{-1} at a GRT of 4 h. Our study demonstrates a higher net MPR of 1.02±0.11 L_{CH4} L_R^{-1} d^{-1} at the same GRT of 4 h under mesophilic conditions, representing a notable 25% increase. This improved performance was achieved with a surprisingly low gas recirculation rate of only 4 L L_R^{-1} h^{-1}, which is 5 times lower than the 20.14 L L_R^{-1} h^{-1} employed by Bassani et al. [48]. Similarly, [20] investigated the efficiency of aluminum oxide gas diffusers, testing various pore sizes in thermophilic BRs. Their results documented a net MPR of

 doi:10.20944/preprints202602.1438.v1

1.30±0.15 L_{CH4} L_R^{-1} d^{-1} at a GRT of 2.5 h and a gas recirculation rate of 4.87 L L_R^{-1} h^{-1}. In comparison, our research achieved a higher net MPR of 1.46±0.06 L_{CH4} L_R^{-1} d^{-1} at a GRT of 2.8 h and a gas recirculation rate of 4 L L_R^{-1} h^{-1}. [22] focused on the impact of packing material in a thermophilic BR, reporting a net MPR of 0.67±0.17 L_{CH4} L_R^{-1} d^{-1} at a GRT of 5 h and a gas recirculation rate of 8.8 L L_R^{-1} h^{-1}. Our study presents comparable results, with a higher net MPR of 0.71±0.01 L_{CH4} L_R^{-1} d^{-1} at a slightly longer GRT of 5.5 h.

Based on previous studies, the performance of BR herein demonstrates an improvement in biomethanation efficiency, highlighting the promising role of bentonite as a cost-effective additive that increases hydrostatic pressure in the mixed liquor. Intriguingly, Luo et al. [18] found that under thermophilic conditions, the H_2 utilization rate increases by 60% compared with mesophilic conditions. However, our findings challenge these expectations, demonstrating that the bioreactor, while operating in the mesophilic range, has exceeded its anticipated performance, highlighting the potential of adding bentonite in the BR.

The notable absence of VFAs at the bentonite-enriched BR is significant, suggesting that hydrogenotrophic methanogenesis was the prevailing process and that the homoacetogenic metabolic pathway of homoacetogenesis was not favored. In contrast, several ex-situ biogas upgrading studies conducted under thermophilic conditions have reported high concentrations of VFAs, raising concerns about the process stability, since they can severely hinder reactor performance and even provoke process inhibition. For instance, Jonson et al. [49] observed VFA levels reaching 2.1 g L_R^{-1}, while Tsapekos et al. [46] documented concentrations as high as 1.2 g L_R^{-1}. At these VFA concentrations, process efficiency was reduced drastically, with the methane content of the biomethane decreasing from 95% to around 70%. While thermophilic systems may be known for their higher reaction rates, they also carry an inherent risk of operational instability, such as the accumulation of VFAs or unpredictable pH fluctuations. In striking contrast, this study's findings demonstrate the stability of mesophilic biomethanation even at low GRTs, a crucial factor for large-scale systems that require reliability and consistency.

Ex-situ biological upgrading of biogas in TBRs is superior to that in BRs. However, the results of the BR in this study during the XI phase (MPR of 2.17±0.06 L_{CH4} L_R^{-1} d^{-1} under a GRT of 1.49 h) are comparable to some studies in the literature focusing on thermophilic TBRs. Sieborg et al. [50] reported a net MPR of 2.08±0.04 L_{CH4} L_R^{-1} d^{-1} at a GRT of 1.32h. [51] reported a net MPR of 1.74±0.01 L_{CH4} L_R^{-1} d^{-1} at a GRT of 2.1 h, which is very similar to the net MPR of 1.81±0.01 L_{CH4} L_R^{-1} d^{-1} at a GRT of 1.98 h found here. However, significantly higher biomethanation rates have been documented in the literature under optimized TBR configurations. Jønson et al. [49] reported a net MPR of 10.6±0.6 L_{CH4} L_R^{-1} d^{-1} at a GRT of approximately 20 min, utilizing a packed material with a high surface area of 3500 m^2/m^3. Similarly, Ashraf et al. [8] achieved a net MPR of 8.54±0.47 L_{CH4} L_R^{-1} d^{-1} using polyurethane foam as a packing medium. Strübing et al. [52] demonstrated that TBR can accomplish a net MPR of 15.4±0.0 L_{CH4} L_R^{-1} d^{-1} with a CH_4 concentration of 98.5±0.7%. These findings indicate that TBRs, when operated under optimal conditions, can achieve a significantly higher hydrogen mass-transfer rate than the BR configuration evaluated in this study. However, it is essential to note that the net MPR is expected to be higher when the feeding gas consists solely of CO_2 and H_2 [8,41]. This contrasts with studies in which the upgrading system is supplied with a mixture of CO_2, H_2, and CH_4 (or a gas simulating biogas CH_4). Therefore, direct comparisons across ex-situ biogas upgrading studies should be interpreted with caution, as differences in gas composition can influence CH_4 production rates.

The higher efficiency of the bioreactor presented in our study can be attributed, in part, to the elevated hydrostatic pressure within the reactor and the increased viscosity of the mixed liquor. Existing research on ex-situ biomethanation has examined the effects of pressure. For example, Ullrich et al. [31] explored the impact of pressures ranging from 1.5 to 9 bar within a thermophilic TBR. Their findings established a clear, positive relationship between applied pressure and methane concentration in the upgraded biogas: the higher the pressure, the richer the biomethane became in CH_4. Similarly, Ebrahimian et al. [21] examined the performance of a thermophilic TBR operating at a mere overpressure of 0.7 bar, revealing the capability to achieve CH_4 concentrations exceeding 90% even with a remarkably short GRT of just 21 min. In the current study, the pressure in the BR was

 doi:10.20944/preprints202602.1438.v1

calculated to be 1.12 bars at the bottom of the reactor and decreased to 1 bar near the headspace. The calculation was based on the slurry mixture's density, as explained in the Materials and Methods section. This is relatively low pressure, which may not be entirely responsible for the BR's high performance.

The enhanced performance of the bentonite-enriched BR can be interpreted as the combined effects of hydrodynamic and microenvironmental factors induced by bentonite in the mixed liquor [53]. The bentonite used in this study consisted predominantly of montmorillonite (≥80% w/w, dry basis), a clay mineral characterized by high swelling capacity and a specific adsorption capacity exceeding 300 mg 100 g^{-1} [38,39]. The resulting increase in slurry density and apparent viscosity likely reduced bubble rise velocity relative to the reference BR, thereby prolonging gas residence time and improving gas–liquid contact. This interpretation is supported by the significantly higher net MPRs and hydrogen utilization efficiencies observed in the bentonite-enriched system, particularly at gas retention times (GRTs) below 10.5 h, where the reference reactor exhibited a clear performance plateau of approximately 0.27 L CH_4 L_R^{-1} d^{-1}.

Beyond hydrodynamic effects, bentonite may also have contributed to enhanced process stability through physicochemical interactions within the liquid phase. The layered aluminosilicate structure of bentonite and its high cation exchange capacity provide extensive surface area for microbial attachment [31,51]. In addition, the mildly alkaline nature of the clay (pH 9.23 in a 5% aqueous dispersion) likely increased the system's buffering capacity, consistent with the stable pH observed throughout the experimental period. Furthermore, the high surface area and ion-exchange properties of montmorillonite offer plausible mechanisms for the adsorption of inhibitory intermediates and the formation of favorable microenvironments that promote hydrogenotrophic methanation [32,35]. The porous, hydrated structure of bentonite may also facilitate diffusion of dissolved gases, enhancing local H_2 and CO_2 availability to methanogenic cells [52]. In this way, bentonite could indirectly support hydrogenotrophic methanogenesis by improving mass transfer within the biofilm–liquid continuum [32,51]. An additional benefit may arise from the mechanical stability imparted by bentonite particles, which can protect attached microorganisms from shear stress [31]. Although direct measurements of gas–liquid mass transfer coefficients or microbial attachment were not conducted, the increased methane productivity, high methane purity, and absence of VFA accumulation at HLRs suggest that bentonite acts as an effective environmental moderator, thereby benefiting ex-situ biological biogas upgrading.

Despite the clear performance enhancement observed in the bentonite-enriched BR, several limitations of the present study must be acknowledged. No direct hydrodynamic characterization was performed for either the reference or bentonite-amended reactors; bubble size distribution, gas holdup profiles, and volumetric mass transfer coefficients (k_La) were not measured. Consequently, the proposed enhancement in mass transfer is inferred from comparative reactor performance. In addition, microbial community analyses were not conducted to confirm microbial attachment to bentonite particles directly. Accordingly, the present work should be regarded as a proof-of-concept, demonstrating that low-cost mineral additives can enhance biomethanation performance in bubble reactors by modifying hydrodynamic and microenvironmental conditions within the mixed liquor.

Future studies should focus on the influence of bentonite type, dosage, and particle size, as well as on directly quantifying mass-transfer parameters and microbial attachment. Further performance improvements may be achieved through operational strategies, such as increasing gas recirculation rates or operating under thermophilic conditions. Such approaches could enable bubble reactors to approach the performance levels reported for TBRs while maintaining operational simplicity.

5. Conclusions

The integration of bentonite into the BR significantly improved biomethanation efficiency, resulting in a net MPR almost twice that of the reference BR at the same HLR. Notably, this enhancement occurred without relying on specialized hydrogen-diffusion mechanisms or increased gas recirculation rates. The peak net MRP was 2.17±0.06 L_{CH4} L_R^{-1} d^{-1} at a GRT of 1.49 h, and the methane content in the resultant biomethane was 96.25%. These findings were achieved under mesophilic conditions, surpassing efficiencies typically reported in thermophilic BR setups.

 doi:10.20944/preprints202602.1438.v1

Throughout the process, pH was maintained between 8.0 and 8.5, which aligns well with optimal conditions for hydrogenotrophic methanogenesis. Bentonite served as a medium to increase the density of the mixed liquor and, therefore, its pressure, and may also have contributed to creating a favorable microenvironment that supports microbial metabolism and stability.

Author Contributions: For research articles with several authors, a short paragraph specifying their individual contributions must be provided. The following statements should be used Conceptualization, A.S. and K.S.; methodology, A.S. and K.S.; investigation, A.S.; data curation, A.S. and K.S.; writing—original draft preparation, A.S.; writing—review and editing, A.S. and K.S.; visualization, A.S. and P.S.; supervision, K.S.; project administration, K.S.; funding acquisition, A.S. All authors have read and agreed to the published version of the manuscript.

Funding: The research work was supported by the Hellenic Foundation for Research and Innovation (HFRI) under the HFRI PhD Fellowship grant (Fellowship Number: 1585).

Data Availability Statement: Experimental data supporting the results are presented in Spyridonidis and Stamatelatou "Enhancing Hydrogenotrophic Methanation in a Bentonite-Amended Bubble Reactor under Mesophilic Conditions" [Data set]. Zenodo. https://doi.org/10.5281/zenodo.18624458.

Acknowledgments: During the preparation of this manuscript/study, the authors used online tools (Grammarly https://app.grammarly.com/, ChatGPT 5.2) to improve the linguistic aspects and to search for relevant literature. The authors have reviewed and edited the output and take full responsibility for the content of this publication.

Conflicts of Interest: The authors declare no conflicts of interest.

Abbreviations

The following abbreviations are used in this manuscript:

BR	Bubble reactor
CH_4	Methane
CLR	Carbon dioxide loading rate
CO_2	Carbon dioxide
COR	Carbon dioxide outlet rate
CSTR	Continuous stirred tank reactor
FOS/TAC	Ratio of volatile organic acids to total inorganic carbonate alkalinity
GHG	Greenhouse gas
GLR	Gas loading rate
GRT	Gas retention time (h)
H_2	Hydrogen
HLR	Hydrogen loading rate (L H_2 L_R^{-1} d^{-1})
HLR_in	Hydrogen inlet loading rate
HOR	Hydrogen outlet rate
k_{LA}	Volumetric gas–liquid mass transfer coefficient
L_R	Reactor working volume (L)
MLR	Methane loading rate
MPR	Methane production rate (L CH_4 L_R^{-1} d^{-1})
N_2	Nitrogen
NH_3-N	Ammoniacal nitrogen
TBR	Trickle bed reactor
TS	Total solids
v/v	Volume per volume
VFAs	Volatile fatty acids
VS	Volatile solids

Appendix A: Characterization of Bentonite and Digestate Used for Inoculation and Nutrient Supplement

 doi:10.20944/preprints202602.1438.v1

Table A1. Characteristics of bentonite.

Parameter	Value
Dry matter (%)	89
pH dispersion 5%	9.23
Extractable Na (g $kgDM^{-1}$)	35
Montmorillonate (g $kgDM^{-1}$)	800
Particles <10 µm	10
Crystalline silica %	3
Specific surface absorption (mg $100g^{-1}$)	300
Disacidifying power (g $kgDM^{-1}$)	2.5

Table A2. Characteristics of inoculum prior to bentonite addition.

Parameter	Value
pH	7.78 ± 0.18
Conductivity @25°C (mS cm^{-1})	17.98 ± 0.23
TS (%)	3.29 ± 0.21
VS (%)	2.61 ± 0.50
NH_3-N (mg L_R^{-1})	1943 ± 32
VFAs	
acetate (mg L_R^{-1})	n.d.
propionate (mg L_R^{-1})	n.d.
isobutyrate (mg L_R^{-1})	n.d.
butyrate (mg L_R^{-1})	n.d.
isovalerate (mg L_R^{-1})	n.d.
valerate (mg L_R^{-1})	n.d.
Total Alkalinity (g $CaCO_3$ L_R^{-1})	10.9
FOS/TAC	0.178
Potassium (%)	2.07
Aluminum (mg $kgDM^{-1}$)	1400
Cadmium (mg $kgDM^{-1}$)	0.3
Cobalt (mg $kgDM^{-1}$)	2.12
Iron (mg $kgDM^{-1}$)	4680
Copper (mg $kgDM^{-1}$)	391
Manganese (mg $kgDM^{-1}$)	500
Molybdenum (mg $kgDM^{-1}$)	8.75
Nickel (mg $kgDM^{-1}$)	17.4
Selenium (mg $kgDM^{-1}$)	0.95
Tungsten (mg $kgDM^{-1}$)	<0.500
Tin (mg $kgDM^{-1}$)	1.29
Zinc (mg $kgDM^{-1}$)	3.57
Phosphorus (mg $kgDM^{-1}$)	3.01

Appendix B: Pressure Calculation

 doi:10.20944/preprints202602.1438.v1

To determine the pressure at the bottom of the BR, the relative density of the total solids was first calculated using the equation B1 [54].

$$\frac{W_s}{S_S \cdot \rho_w} = \frac{W_f}{S_f \cdot \rho_w} + \frac{W_v}{S_v \cdot \rho_w} \quad \textbf{(Eq. B1)}$$

where:
W_s = total solids weight (21.9 g per 100 g of sludge)
S_S = relative density of total solids (dimensionless)
ρ_w = water density (1000 g Lκ^{-1})
W_v = volatile solids weight (2.3 g per 100 g of sludge)
S_v = relative density of volatile solids (1, typical value)
W_f = total fixed solids weight (21.9-2.3=19.6 g per 100 g of sludge)
S_f = relative density of total fixed solids (2.5, typical value)

$$S_S = 2.16$$

Similarly, the relative density of mixed liquor (sludge) was calculated based on the equation (Eq. B2).

$$\frac{W_{sl}}{S_{Sl} \cdot \rho_w} = \frac{W_s}{S_s \cdot \rho_w} + \frac{W_w}{S_w \cdot \rho_w} \quad \textbf{(Eq. B2)}$$

where:
W_{sl} = total sludge weight (100 g)
S_{Sl} = relative density of sludge
W_w = total weight of sludges' water (100-21.9=78.1 g)
S_w = relative density of water (1)

$$S_{Sl} = 1.133$$

The pressure developed at the bottom of the BR is calculated via the equation (Eq. B3).

$$P = P_{atm} + \rho_{sl} \cdot g \cdot h \quad \textbf{(Eq. B3)}$$

where:
P_{atm} =101325 Pa
ρ_{sl} = sludge density ($S_{Sl} \cdot \rho_w = 1.134 \cdot 1000 = 1134$ g L^{-1})
g = gravitational accelaration constant (9.81 m s-2)
h = height of mixed liquor (1 m)

$$P \cong 1.12\text{bar}$$

References

1. Feickert Fenske, C.; Kirzeder, F.; Strübing, D.; Koch, K. Biogas Upgrading in a Pilot-Scale Trickle Bed Reactor – Long-Term Biological Methanation under Real Application Conditions. *Bioresource Technology* **2023**, *376*, 128868, doi:10.1016/j.biortech.2023.128868.
2. Charalambous, P.; Constantinou, D.; Samanides, C.G.; Vyrides, I. Enhancing Biogas Production from Cheese Whey Using Zero-Valent Iron: A Comparative Analysis of Batch and Semi-Continuous Operation Modes. *Journal of Environmental Chemical Engineering* **2023**, *11*, 111278, doi:10.1016/j.jece.2023.111278.
3. Feickert Fenske, C.; Md, Y.; Strübing, D.; Koch, K. Preliminary Gas Flow Experiments Identify Improved Gas Flow Conditions in a Pilot-Scale Trickle Bed Reactor for H2 and CO2 Biological Methanation. *Bioresource Technology* **2023**, *371*, 128648, doi:10.1016/j.biortech.2023.128648.
4. Chen, L.; Du, S.; Xie, L. Effects of pH on Ex-Situ Biomethanation with Hydrogenotrophic Methanogens under Thermophilic and Extreme-Thermophilic Conditions. *Journal of Bioscience and Bioengineering* **2021**, *131*, 168–175, doi:10.1016/j.jbiosc.2020.09.018.

5. Feickert Fenske, C.; Strübing, D.; Koch, K. Biological Methanation in Trickle Bed Reactors - a Critical Review. *Bioresource Technology* **2023**, *385*, 129383, doi:10.1016/j.biortech.2023.129383.
6. Giuliano, A.; Cellamare, C.M.; Chiarini, L.; Tabacchioni, S.; Petta, L. Evaluation of the Controlled Hydrodynamic Cavitation as Gas Mass Transfer System for Ex-Situ Biological Hydrogen Methanation. *Chemical Engineering Journal* **2023**, *471*, 144475, doi:10.1016/j.cej.2023.144475.
7. Agneessens, L.M.; Ottosen, L.D.M.; Andersen, M.; Berg Olesen, C.; Feilberg, A.; Kofoed, M.V.W. Parameters Affecting Acetate Concentrations during In-Situ Biological Hydrogen Methanation. *Bioresource Technology* **2018**, *258*, 33–40, doi:10.1016/j.biortech.2018.02.102.
8. Ashraf, M.T.; Sieborg, M.U.; Yde, L.; Rhee, C.; Shin, S.G.; Triolo, J.M. Biomethanation in a Thermophilic Biotrickling Filter — pH Control and Lessons from Long-Term Operation. *Bioresource Technology Reports* **2020**, *11*, 100525, doi:10.1016/j.biteb.2020.100525.
9. Spyridonidis, A.; Vasiliadou, I.A.; Stathopoulou, P.; Tsiamis, A.; Tsiamis, G.; Stamatelatou, K. Enrichment of Microbial Consortium with Hydrogenotrophic Methanogens for Biological Biogas Upgrade to Biomethane in a Bubble Reactor under Mesophilic Conditions. *Sustainability* **2023**, *15*, 15247, doi:10.3390/su152115247.
10. Francisco López, A.; Lago Rodríguez, T.; Faraji Abdolmaleki, S.; Galera Martínez, M.; Bello Bugallo, P.M. From Biogas to Biomethane: An In-Depth Review of Upgrading Technologies That Enhance Sustainability and Reduce Greenhouse Gas Emissions. *Applied Sciences* **2024**, *14*, 2342, doi:10.3390/app14062342.
11. Kozak, M.; Köroğlu, E.O.; Cirik, K.; Zaimoğlu, Z. Evaluation of Ex-Situ Hydrogen Biomethanation at Mesophilic and Thermophilic Temperatures. *International Journal of Hydrogen Energy* **2022**, *47*, 15434–15441, doi:10.1016/j.ijhydene.2022.02.072.
12. Angelidaki, I.; Treu, L.; Tsapekos, P.; Luo, G.; Campanaro, S.; Wenzel, H.; Kougias, P.G. Biogas Upgrading and Utilization: Current Status and Perspectives. *Biotechnology Advances* **2018**, *36*, 452–466, doi:10.1016/j.biotechadv.2018.01.011.
13. Sposob, M.; Wahid, R.; Fischer, K. Ex-Situ Biological CO2 Methanation Using Trickle Bed Reactor: Review and Recent Advances. *Rev Environ Sci Biotechnol* **2021**, *20*, 1087–1102, doi:10.1007/s11157-021-09589-7.
14. Huang, J.-H.; Fan, X.-L.; Li, R.; Sun, M.-T.; Zou, H.; Zhang, Y.-F.; Guo, R.-B.; Fu, S.-F. Biogas Upgrading by Biotrickling Filter: Effects of Temperature and Packing Materials. *Chemical Engineering Journal* **2024**, *481*, 148367, doi:10.1016/j.cej.2023.148367.
15. Sposób, M. Optimization of Ex-Situ Biomethanation Process in Trickle Bed Reactor: The Impact of Slight H2/CO2 Ratio Adjustments and Different Packing Materials. *Renewable Energy* **2024**, *222*, 119971, doi:10.1016/j.renene.2024.119971.
16. Rao, Y.; Chibwe, K.; Mantilla-Calderon, D.; Ling, F.; He, Z. Meta-Analysis of Biogas Upgrading to Renewable Natural Gas through Biological CO2 Conversion. *Journal of Cleaner Production* **2023**, *426*, 139128, doi:10.1016/j.jclepro.2023.139128.
17. Mares, S.; Moreno-Andrade, I.; Quijano, G. Biological CH4 Production from H2/CO2 Streams: Influence of Trace Metals Concentration on the Hydrogenotrophic Process. *Journal of Environmental Chemical Engineering* **2023**, *11*, 109528, doi:10.1016/j.jece.2023.109528.
18. Luo, G.; Angelidaki, I. Integrated Biogas Upgrading and Hydrogen Utilization in an Anaerobic Reactor Containing Enriched Hydrogenotrophic Methanogenic Culture. *Biotech & Bioengineering* **2012**, *109*, 2729–2736, doi:10.1002/bit.24557.
19. Kougias, P.G.; Treu, L.; Benavente, D.P.; Boe, K.; Campanaro, S.; Angelidaki, I. Ex-Situ Biogas Upgrading and Enhancement in Different Reactor Systems. *Bioresource Technology* **2017**, *225*, 429–437, doi:10.1016/j.biortech.2016.11.124.
20. Ghofrani-Isfahani, P.; Tsapekos, P.; Peprah, M.; Kougias, P.; Zhu, X.; Kovalovszki, A.; Zervas, A.; Zha, X.; Jacobsen, C.S.; Angelidaki, I. Ex-Situ Biogas Upgrading in Thermophilic up-Flow Reactors: The Effect of Different Gas Diffusers and Gas Retention Times. *Bioresource Technology* **2021**, *340*, 125694, doi:10.1016/j.biortech.2021.125694.
21. Ebrahimian, F.; De Bernardini, N.; Tsapekos, P.; Treu, L.; Zhu, X.; Campanaro, S.; Karimi, K.; Angelidaki, I. Effect of Pressure on Biomethanation Process and Spatial Stratification of Microbial Communities in

Trickle Bed Reactors under Decreasing Gas Retention Time. *Bioresource Technology* **2022**, *361*, 127701, doi:10.1016/j.biortech.2022.127701.

22. Kougias, P.G.; Tsapekos, P.; Treu, L.; Kostoula, M.; Campanaro, S.; Lyberatos, G.; Angelidaki, I. Biological CO2 Fixation in Up-Flow Reactors via Exogenous H2 Addition. *Journal of Biotechnology* **2020**, *319*, 1–7, doi:10.1016/j.jbiotec.2020.05.012.
23. Ghofrani-Isfahani, P.; Tsapekos, P.; Peprah, M.; Kougias, P.; Zervas, A.; Zhu, X.; Yang, Z.; Jacobsen, C.S.; Angelidaki, I. Ex-Situ Biogas Upgrading in Thermophilic Trickle Bed Reactors Packed with Micro-Porous Packing Materials. *Chemosphere* **2022**, *296*, 133987, doi:10.1016/j.chemosphere.2022.133987.
24. Chatzis, A.; Orellana, E.; Gaspari, M.; Kontogiannopoulos, K.; Treu, L.; Zouboulis, A.; Kougias, P.G. Comparative Study on Packing Materials for Improved Biological Methanation in Trickle Bed Reactors. *Bioresource Technology* **2023**, *385*, 129456, doi:10.1016/j.biortech.2023.129456.
25. Spyridonidis, A.; Stamatelatou, K. Comparative Study of Mesophilic Biomethane Production in Ex Situ Trickling Bed and Bubble Reactors. *Fermentation* **2024**, *10*, 554, doi:10.3390/fermentation10110554.
26. Burkhardt, M.; Jordan, I.; Heinrich, S.; Behrens, J.; Ziesche, A.; Busch, G. Long Term and Demand-Oriented Biocatalytic Synthesis of Highly Concentrated Methane in a Trickle Bed Reactor. *Applied Energy* **2019**, *240*, 818–826, doi:10.1016/j.apenergy.2019.02.076.
27. Karyofyllidou, C.; Spyridonidis, A.; Diamantis, V.; Galiatsatos, I.; Tsiamis, G.; Stathopoulou, P.; Kosmadakis, I.; Eftaxias, A.; Stamatelatou, K. Mesophilic Trickle-Bed Reactors for Enhanced Ex Situ Biogas Upgrading at Short Gas Retention Times: Process Performance and Microbial Insights. *Fermentation* **2026**, *12*, 69, doi:10.3390/fermentation12020069.
28. Jensen, M.B.; Poulsen, S.; Jensen, B.; Feilberg, A.; Kofoed, M.V.W. Selecting Carrier Material for Efficient Biomethanation of Industrial Biogas-CO2 in a Trickle-Bed Reactor. *Journal of CO2 Utilization* **2021**, *51*, 101611, doi:10.1016/j.jcou.2021.101611.
29. Trejo-Aguilar, G.; Revah, S.; Lobo-Oehmichen, R. Hydrodynamic Characterization of a Trickle Bed Air Biofilter. *Chemical Engineering Journal* **2005**, *113*, 145–152, doi:10.1016/j.cej.2005.04.001.
30. Burkhardt, M.; Koschack, T.; Busch, G. Biocatalytic Methanation of Hydrogen and Carbon Dioxide in an Anaerobic Three-Phase System. *Bioresource Technology* **2015**, *178*, 330–333, doi:10.1016/j.biortech.2014.08.023.
31. Ullrich, T.; Lindner, J.; Bär, K.; Mörs, F.; Graf, F.; Lemmer, A. Influence of Operating Pressure on the Biological Hydrogen Methanation in Trickle-Bed Reactors. *Bioresource Technology* **2018**, *247*, 7–13, doi:10.1016/j.biortech.2017.09.069.
32. Rittmann, B.E.; McCarty, P.L. *Environmental Biotechnology: Principles and Applications*; McGraw-Hill Education: New York, N.Y., 2018; ISBN 978-1-260-44059-1.
33. Saini, S.; Tewari, S.; Dwivedi, J.; Sharma, V. Biofilm-Mediated Wastewater Treatment: A Comprehensive Review. *Mater. Adv.* **2023**, *4*, 1415–1443, doi:10.1039/D2MA00945E.
34. Zhao, T.; Chen, Y.; Yu, Q.; Shi, D.; Chai, H.; Li, L.; Ai, H.; Gu, L.; He, Q. Enhancement of Performance and Stability of Anaerobic Co-Digestion of Waste Activated Sludge and Kitchen Waste by Using Bentonite. *PLoS ONE* **2019**, *14*, e0218856, doi:10.1371/journal.pone.0218856.
35. Yun, Y.-M.; Sung, S.; Kang, S.; Kim, M.-S.; Kim, D.-H. Enrichment of Hydrogenotrophic Methanogens by Means of Gas Recycle and Its Application in Biogas Upgrading. *Energy* **2017**, *135*, 294–302, doi:10.1016/j.energy.2017.06.133.
36. Hu, F.; Zhang, S.; Liu, S.; Wan, L.; Gong, G.; Hu, T.; Wang, X.; Xu, L.; Xu, G.; Hu, Y. Alleviating Acid Inhibition via Bentonite Supplementation during Acidulated Swine Manure Anaerobic Digestion: Performance Enhancement and Microbial Mechanism Analysis. *Chemosphere* **2023**, *313*, 137577, doi:10.1016/j.chemosphere.2022.137577.
37. Tzenos, C.A.; Kalamaras, S.D.; Economou, E.-A.; Romanos, G.Em.; Veziri, C.M.; Mitsopoulos, A.; Menexes, G.C.; Sfetsas, T.; Kotsopoulos, T.A. The Multifunctional Effect of Porous Additives on the Alleviation of Ammonia and Sulfate Co-Inhibition in Anaerobic Digestion. *Sustainability* **2023**, *15*, 9994, doi:10.3390/su15139994.
38. Odom, I.E. Smectite Clay Minerals: Properties and Uses. *Phil. Trans. R. Soc. Lond. A* **1984**, 391–409.

39. Heller, H.; Keren, R. Rheology of Na-Rich Montmorillonite Suspension as Affected by Electrolyte Concentration and Shear Rate. *Clays and clay miner.* **2001**, *49*, 286–291, doi:10.1346/CCMN.2001.0490402.
40. Du, W.; Yang, Y.; Hu, L.; Chang, B.; Cao, G.; Nasir, M.; Lv, J. Combined Determination Analysis of Surface Properties Evolution towards Bentonite by pH Treatments. *Colloids and Surfaces A: Physicochemical and Engineering Aspects* **2021**, *626*, 127067, doi:10.1016/j.colsurfa.2021.127067.
41. Zhang, S.; Tan, D.; Zhu, H.; Pei, H.; Shi, B. Rheological Behaviors of Na-Montmorillonite Considering Particle Interactions: A Molecular Dynamics Study. *Journal of Rock Mechanics and Geotechnical Engineering* **2025**, *17*, 4657–4671, doi:10.1016/j.jrmge.2024.07.003.
42. Alfaro, N.; Fdz-Polanco, M.; Fdz-Polanco, F.; Díaz, I. Evaluation of Process Performance, Energy Consumption and Microbiota Characterization in a Ceramic Membrane Bioreactor for Ex-Situ Biomethanation of H2 and CO2. *Bioresource Technology* **2018**, *258*, 142–150, doi:10.1016/j.biortech.2018.02.087.
43. Rachbauer, L.; Voitl, G.; Bochmann, G.; Fuchs, W. Biological Biogas Upgrading Capacity of a Hydrogenotrophic Community in a Trickle-Bed Reactor. *Applied Energy* **2016**, *180*, 483–490, doi:10.1016/j.apenergy.2016.07.109.
44. Lee, J.C.; Kim, J.H.; Chang, W.S.; Pak, D. Biological Conversion of CO2 to CH4 Using Hydrogenotrophic Methanogen in a Fixed Bed Reactor. *J. Chem. Technol. Biotechnol.* **2012**, *87*, 844–847, doi:10.1002/jctb.3787.
45. Kamravamanesh, D.; Rinta Kanto, J.M.; Ali-Loytty, H.; Myllärinen, A.; Saalasti, M.; Rintala, J.; Kokko, M. Ex-Situ Biological Hydrogen Methanation in Trickle Bed Reactors: Integration into Biogas Production Facilities. *Chemical Engineering Science* **2023**, *269*, 118498, doi:10.1016/j.ces.2023.118498.
46. Tsapekos, P.; Treu, L.; Campanaro, S.; Centurion, V.B.; Zhu, X.; Peprah, M.; Zhang, Z.; Kougias, P.G.; Angelidaki, I. Pilot-Scale Biomethanation in a Trickle Bed Reactor: Process Performance and Microbiome Functional Reconstruction. *Energy Conversion and Management* **2021**, *244*, 114491, doi:10.1016/j.enconman.2021.114491.
47. Thapa, A.; Park, J.-G.; Jun, H.-B. Enhanced Ex-Situ Biomethanation of Hydrogen and Carbon Dioxide in a Trickling Filter Bed Reactor. *Biochemical Engineering Journal* **2022**, *179*, 108311, doi:10.1016/j.bej.2021.108311.
48. Bassani, I.; Kougias, P.G.; Treu, L.; Porté, H.; Campanaro, S.; Angelidaki, I. Optimization of Hydrogen Dispersion in Thermophilic Up-Flow Reactors for Ex Situ Biogas Upgrading. *Bioresource Technology* **2017**, *234*, 310–319, doi:10.1016/j.biortech.2017.03.055.
49. Jønson, B.D.; Tsapekos, P.; Tahir Ashraf, M.; Jeppesen, M.; Ejbye Schmidt, J.; Bastidas-Oyanedel, J.-R. Pilot-Scale Study of Biomethanation in Biological Trickle Bed Reactors Converting Impure CO2 from a Full-Scale Biogas Plant. *Bioresource Technology* **2022**, *365*, 128160, doi:10.1016/j.biortech.2022.128160.
50. Sieborg, M.U.; Jønson, B.D.; Ashraf, M.T.; Yde, L.; Triolo, J.M. Biomethanation in a Thermophilic Biotrickling Filter Using Cattle Manure as Nutrient Media. *Bioresource Technology Reports* **2020**, *9*, 100391, doi:10.1016/j.biteb.2020.100391.
51. Porté, H.; Kougias, P.G.; Alfaro, N.; Treu, L.; Campanaro, S.; Angelidaki, I. Process Performance and Microbial Community Structure in Thermophilic Trickling Biofilter Reactors for Biogas Upgrading. *Science of The Total Environment* **2019**, *655*, 529–538, doi:10.1016/j.scitotenv.2018.11.289.
52. Strübing, D.; Huber, B.; Lebuhn, M.; Drewes, J.E.; Koch, K. High Performance Biological Methanation in a Thermophilic Anaerobic Trickle Bed Reactor. *Bioresource Technology* **2017**, *245*, 1176–1183, doi:10.1016/j.biortech.2017.08.088.
53. Vishnyakova, A.; Popova, N.; Artemiev, G.; Botchkova, E.; Litti, Y.; Safonov, A. Effect of Mineral Carriers on Biofilm Formation and Nitrogen Removal Activity by an Indigenous Anammox Community from Cold Groundwater Ecosystem Alone and Bioaugmented with Biomass from a "Warm" Anammox Reactor. *Biology* **2022**, *11*, 1421, doi:10.3390/biology11101421.
54. *Wastewater Engineering: Treatment and Resource Recovery*; Tchobanoglous, G., Stensel, D.H., Tsuchihashi, R., Burton, F., Abu-Orf, M., Bowden, G., Pfrang, W., Metcalf & Eddy, Inc, Albert Einstein College of Medicine, Eds.; Fifth Edition.; McGraw-Hill Education: New York, 2014; ISBN 978-0-07-340118-8.

 doi:10.20944/preprints202602.1438.v1

disclaim responsibility for any injury to people or property resulting from any ideas, methods, instructions or products referred to in the content.